

## THEORETICAL AND EXPERIMENTAL INVESTIGATION OF FLOW IN A HYDROCYCLONE FOR LIQUID/LIQUID SEPARATION

Carlos Alberto Capela Moraes, [capela@petrobras.com.br](mailto:capela@petrobras.com.br)

Luiz Philipe Martinez Marins, [philipe@petrobras.com.br](mailto:philipe@petrobras.com.br)  
PETROBRAS

João Américo Aguirre Oliveira Jr, [aguirre@esss.com.br](mailto:aguirre@esss.com.br)  
ESSS

Daniel Greco Duarte, [danielgreco@uol.com.br](mailto:danielgreco@uol.com.br)  
UFRJ

**Abstract.** This article describes some comparative results of direct measurements and CFD simulation of the velocity field in a commercial hydrocyclone for oil and water separation, operating with water only. Stereo Particle Image Velocimetry measurements were taken from a transparent acrylic resin prototype of the liquid/liquid hydrocyclone fed with a monophasic water flow, with fixed feed flow rate and pressure drop ratio (pressure drop from inlet to overflow divided by pressure from inlet to underflow). The geometric configuration and boundary conditions of the experimental apparatus were reproduced in the simulation. 3D-Transient Simulation was performed using ANSYS CFX® 11.0 software considering SSG Reynolds Stress Turbulence Model.

**Keywords:** Hydrocyclone, Turbulence, PIV-Particle Image Velocimetry, CFD.

### 1. INTRODUCTION

There is a tendency of increasing the use of hydrocyclones as separation equipment in petroleum production facilities due to its high efficiency and compactness when compared to traditional gravity separation equipment. These characteristics are very much useful in offshore environment where footprint area and load capacity usually mean very high investment costs. Nowadays the use of hydrocyclones in treatment of oily water is very common in offshore installations, but, due to the abovementioned features, their use as oil/water separation in higher oil content process streams is starting to grow.

Despite of its geometric simplicity, hydrocyclones present some challenging characteristics, considering the hydrodynamic and separation performance designs. Some of the features of the flow inside a hydrocyclone pose complex problems to design engineers. Very high fluid velocity, strong centrifugal field, curved streamlines, anisotropic turbulence are some of the characteristics of the flow in a hydrocyclone.

This paper presents some results obtained from direct measurement, using Laser Doppler Anemometer (LDA) and Particle Image Velocimetry (PIV) performed on a commercial hydrocyclone and also results from numerical simulation using CFD software (ANSYS CFX® 11.0) of the same hydrocyclone subject to the same boundary conditions of the experiments. Experimental and numerical results are compared and discussed.

### 2. DESCRIPTION OF THE HYDROCYCLONE

A real scale prototype of one commercial Bulk Oil/Water Cyclone™ from Kvaerner, made of transparent acrylic, was built in order to make possible laser investigation of internal flow. Main geometric characteristics of the prototype can be seen in Fig. 1.

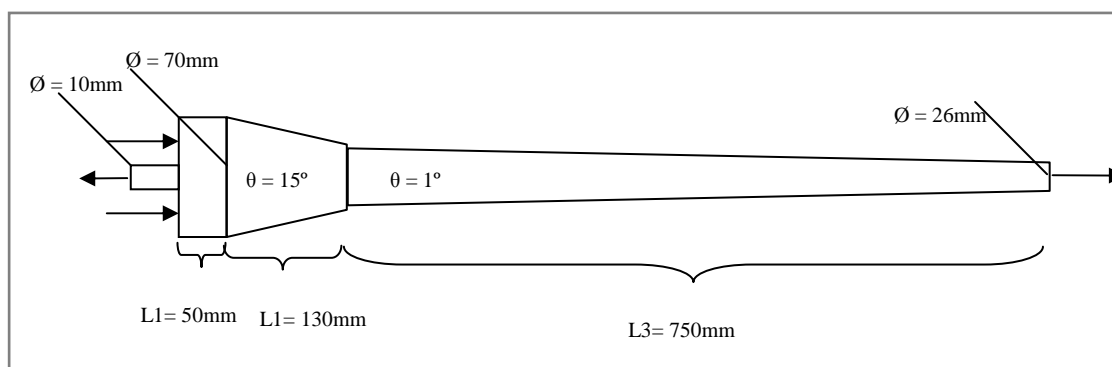


Figure 1. Kvaerner BOW™ Hydrocyclone.

This kind of hydrocyclone was developed by Kvaerner but it is still not in large use in oil production systems. It aims to replace the conventional huge oil/water gravity separators when produced water in feed stream is above 50% of the total liquid (oil+water). Due to its compactness, its use might be advantageous in offshore installations and particularly as a debottleneck device in existing production plants where produced water has increased beyond plant capacity.

### 3. DESCRIPTION OF EXPERIMENTAL RIG AND MEASURING EQUIPMENT

#### 3.1. Description of rig flow diagram

A closed circuit of single phase water flow was assembled so as to feed the prototype with a specified flow rate. The inlet pressure and the two outlet pressures (overflow and underflow) were continuously registered. Fig. 2 below shows a sketch of the flow diagram of the experimental circuit.

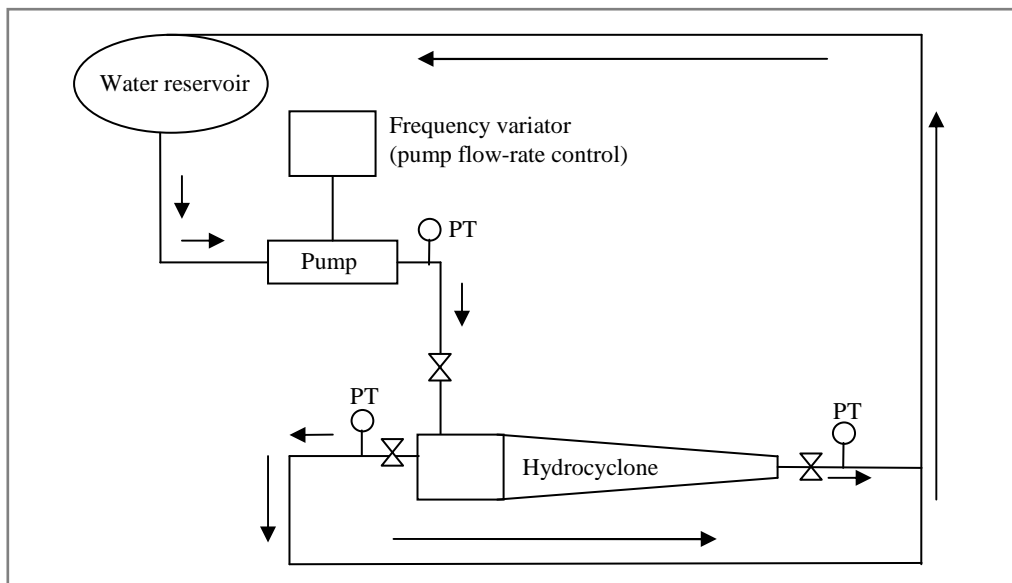


Figure 2. Flow diagram of the experimental rig.

#### 3.2. LDA system configuration

LDA used is a TSI model with two channels with a 5W power argon laser. Characteristics of the laser beams are shown in Tab. 1 and the probe in operation is seen in Fig. 3.

Table 1. LDA laser beams characteristics.

Property	Channel 1	Channel 2
Wave length (nm)	514.5	488
Focal distance (nm)	261.3	261.3
Distance between beams ( $\mu\text{m}$ )	2.70	2.56
Control volume ( $\mu\text{m}$ )	64.59	61.27

#### 3.3. PIV system configuration

PIV system used is from LA Vision with the following characteristics:

- Stereo system – 3 components:  $V_x$ ,  $V_y$ ,  $V_z$ ;
- Two 12 bit cameras w/ 1376 x 1040 pixels of resolution – angle between them =  $75^\circ$ ;
- AF Nikkor 120 mm f/2.8 mm lenses;
- 3-D Calibration target (25 mm x 25 mm);
- Reflexive particles (coated glass beads) – Avg. diameter  $14 \mu\text{m}$ ;
- Nd:YAG BigSky Ultra PIV-120 laser.

PIV system in operation can be seen in Fig. 4, below.

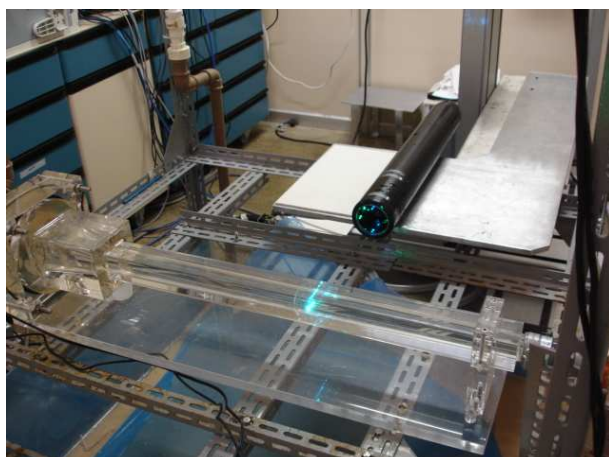


Figure 3. Prototype and LDA probe in operation.

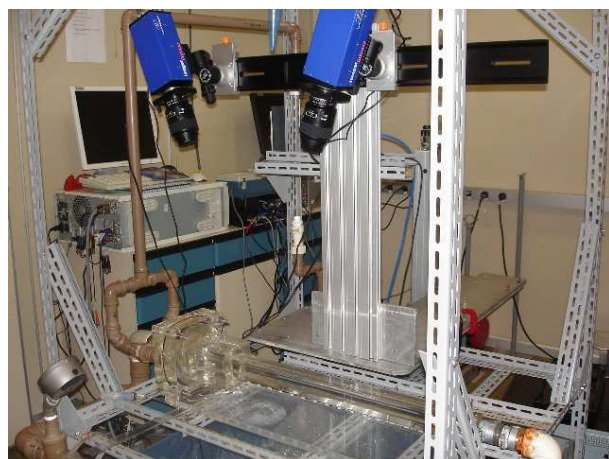


Figure 4. Prototype and PIV cameras.

#### 4. NUMERICAL SIMULATION: GEOMETRY, MESH AND SET-UP

Numerical simulation of the flow inside of a hydrocyclone is already being done by this group with success. Currently, this tool is used to compare different hydrocyclone models, proposed during the design phase. Comparison is based in operation parameters (velocity profiles, mass flow rate, head losses, mass split, etc.) acquired from the simulation results. This is possible since previously a long study about the simulation set-up (mesh parameters, turbulence models, among others) was done, reaching an adequate methodology (Aguirre Oliveira Jr. et al., 2006).

As already mentioned, the CFD software package used is the ANSYS CFX® 11.0. In a few words, CFX is a general-purpose CFD code to approximately solve the conservation equations applying the Element-based Finite Volume method (EbFVm). In this system, around each node of the finite-element mesh a polyhedric control volume is formed. The operations within this control volume have high accuracy given the large number of integration point inside of it. The linearized system of equations is solved using an Algebraic Multi-Grid method (AMG). Detailed information on the governing equations, physical models and numerical methods used can be found in the ANSYS CFX® 11.0 documentation.

##### 4.1. Simulation domain (geometry) and discretization

The geometry of the simulation was built based on the prototype assembly drawings. To assure coherence between physical construction and simulation domain, the whole assembly was reproduced in a CAD interface. This assembly includes the feed involute and the hydrocyclone body. The simulation domain was extracted from the assembly as the cavity space inside of it. Figure 5 shows the modeled geometry (physical assembly and the hydrocyclone involute in detail). Figure 6 shows the simulation domain extracted from the solid assembly, it shows the feed channels, the involute, the hydrocyclone body and the overflow outlet.

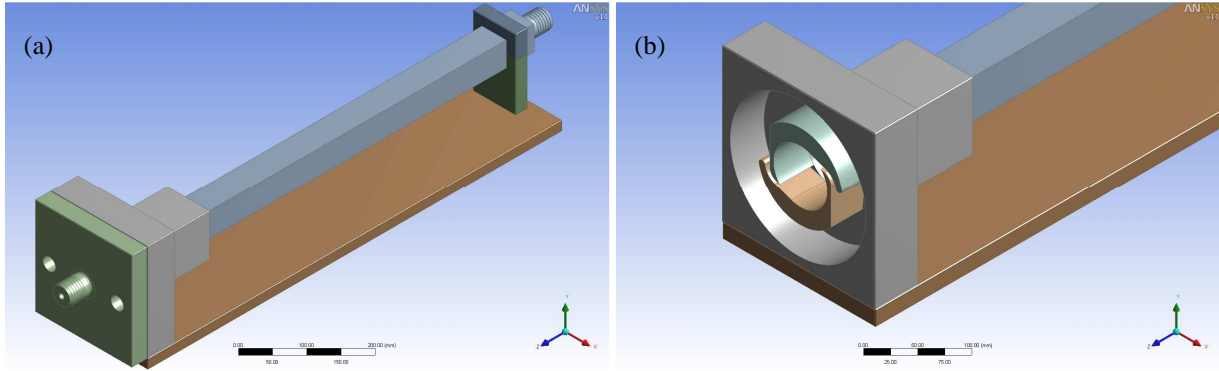


Figure 5. (a) General view and; (b) Feed involute detail.

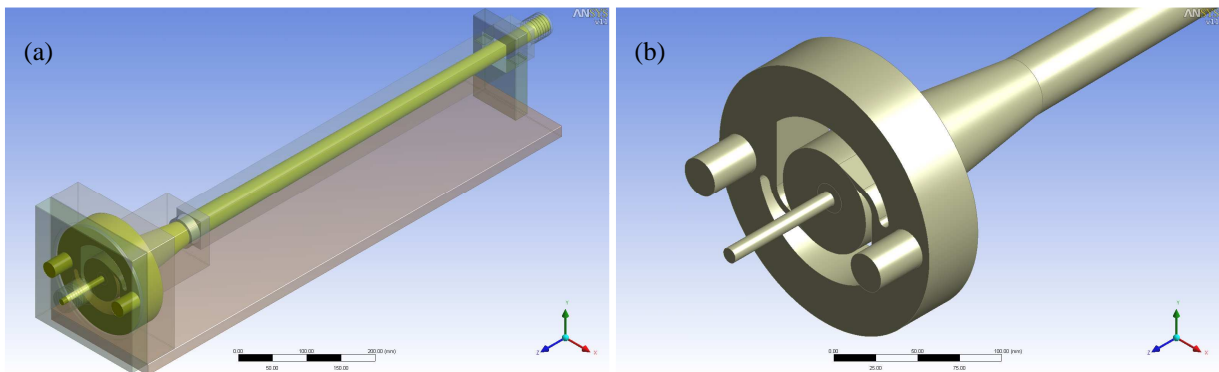


Figure 6. (a) Domain simulation extracted from the assembled model and; (b) Simulation domain involute detail.

In an initial battery of tests this domain was simplified eliminating the external involute and using the channels that link the involute and the hydrocyclone body as the feed condition. In the discretization of the domain, a hexahedral elements mesh was used. Mesh refinements were applied near the walls, in all geometric transitions and in the vortex core region. These refinements are used to capture the effects of the boundary layer and the physical phenomena in the hydrocyclone flow (free and forced vortices, vortex core precessing, etc.). A general view of the mesh and a detailed view of the hydrocyclone body mesh are shown in Fig. 7.

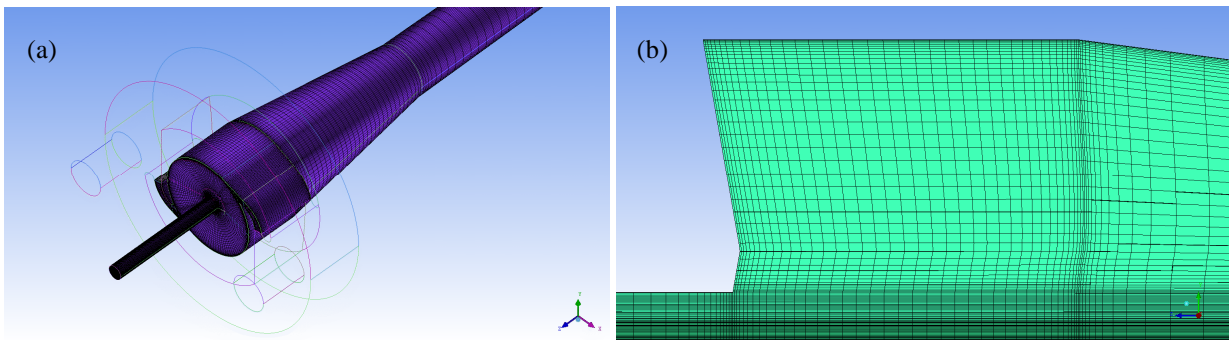


Figure 7. (a) General view and; (b) Hydrocyclone body detail.

The final mesh is consisted of 1999124 elements with a total of 2030334 nodes. The mesh is build using the ANSYS ICEM CFD® 11.0 software. All mesh criteria (quality, aspect ratio, angles, etc.) are kept inside the recommended ranges.

#### 4.3. Simulation set-up

A transient simulation is performed in order to capture the complex phenomena present in the flow. The maximum time step that can be used for this simulation is calculated using Eq. (1) (Montavon et al., 2000). Values above this can cause loss of physical information in the simulation results.

$$\Delta t_{max} = \frac{\min(\phi_{overflow}, \phi_{underflow})}{10 \cdot |U|_{inlet}} \tag{1}$$

Here  $\phi_{overflow}$  and  $\phi_{underflow}$  are the overflow and underflow diameter values. The factor of 10 was introduced because of the high sensitivity of the turbulence models in this case. The simulation time step is adaptative and is allowed to decrease to 1% of the value calculated using Eq. (1).

The boundary conditions imposed are: prescribed mass flow rate in the involute feed (inlet); prescribed mass flow rate in the end of overflow and underflow interfaces (weighted by the mass split) and; no slip condition in the walls. For the turbulence modeling the SSG model (Reynolds Stress model with second-order pressure-strain correlation) was used.

The characteristic time of the flow, taken as being the ratio of the hydrocyclone body volume and the volumetric flow rate, is calculated. After reaching one characteristic time, arithmetic averages of velocity components and pressure are started and reported in the final results file. A convergence criterion of 1.0E-5 (in the RMS error) is adopted for each time step and a mass conservation tolerance of 1% is accepted in the solution.

The problem was executed in five nodes of a cluster, each node composed by two AMD Opteron 275 dual-core processor machines with 16 GB of RAM memory. The simulation took three to four weeks to conclude.

## 5. MEASURING PROCEDURES

### 5.1. LDA procedures

The prototype was built with flat external walls. This approach was used in order to minimize the effects of diffraction and refraction of the laser beams because they have to travel through distinct medium (air, acrylic and water). Even so, it was necessary to make some corrections to correlate external displacement of the probe with the correct internal position of the measuring volume.

Measurements were made in six cross sections of the hydrocyclone, three of them in the 15° tapered cone and three in the 1° tapered cone. Positions of these measuring stations are shown in Fig. 8.

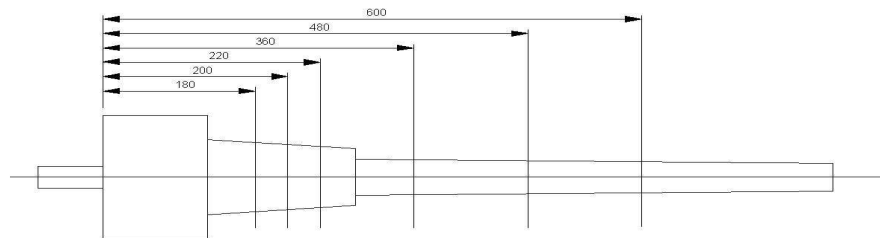


Figure 8. Positions of the measuring stations with LDA.

### 5.1. PIV procedures

Aiming good resolution of the velocity field the cameras were positioned at a 75° angle and the laser sheet was sized to 1 mm thickness. The parameters of the PIV system were adjusted as follows:

- Time between pulses = 18 μs;
- Multipass grid from 64 x 64 pixels and 50% overlap to 32 x 32 pixels and 50% overlap;
- Number of acquired images = 200;
- System set to calculate instantaneous and averaged velocities.

Due to these figures, the investigation strips on axial plane of flow had a length of 50 mm.

## 6. EXPERIMENTAL RESULTS

### 6.1. Operational conditions

The operational conditions used in the experimental tests were defined by the feed flow to the prototype, measured by a rotameter located in the upstream line, and by the pressures measured in all the lines (feed, overflow and underflow lines). The values are shown in Tab. 2.

Table 2. Operational conditions.

Feed flow rate	6.5 m <sup>3</sup> /h
Feed line pressure	346.2 kPa
Overflow line pressure	112.8 kPa
Underflow line pressure	202.0 kPa

The flow split value to the model was estimated, based on the head loss ratio (the inlet-overflow head loss divided by the inlet-underflow head loss), as 35% (35% of the feed flow is directed to the overflow).

### 6.2. Measures velocity profiles

Due to lack of space the measurements of only three stations are show here, the first one in the 15° tapered cone, the second one in the initial portion of the 1° tapered cone the third one in the final portion of the 1° tapered cone. Figure 9 shows the LDV measurement results for the tangential and axial velocity profiles at the first measurement station (at z=180mm). Figures 10 and 11 show the measured velocity profiles by both techniques (LDV and PIV).

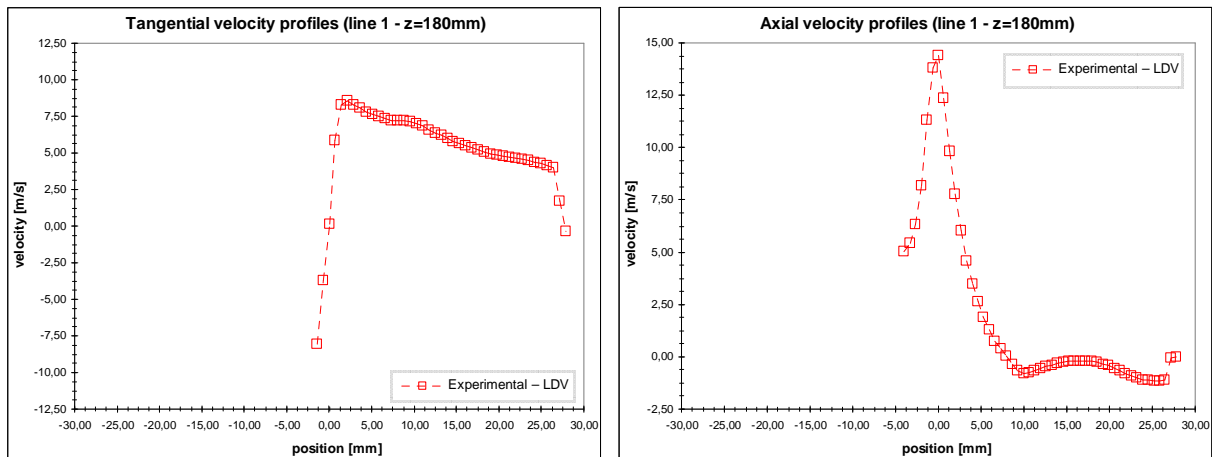


Figure 9. Tangential and axial velocity profiles measured by the LDV probes, station at z=180mm.

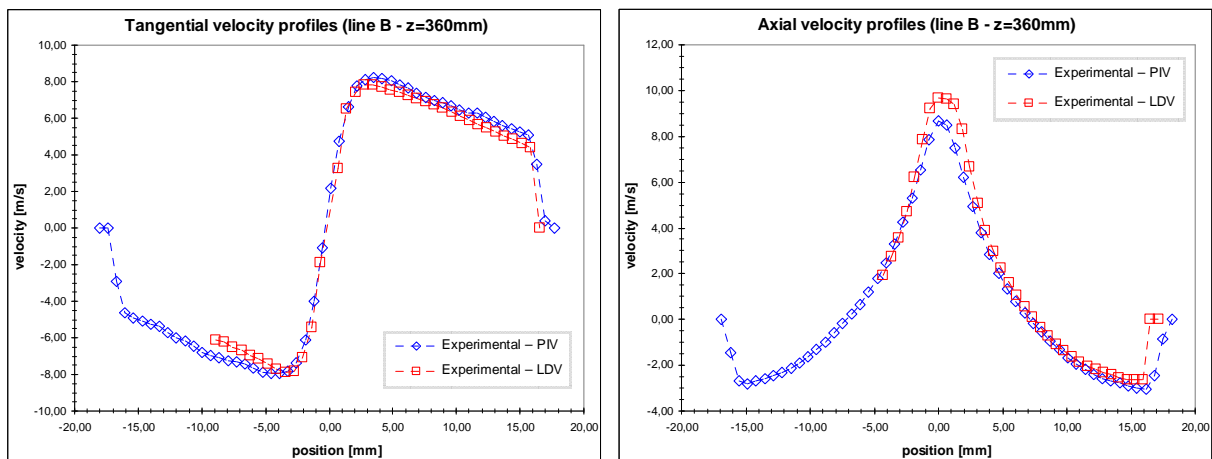


Figure 10. Tangential and axial velocity profiles measured with LDV and PIV techniques, station at z=360mm.

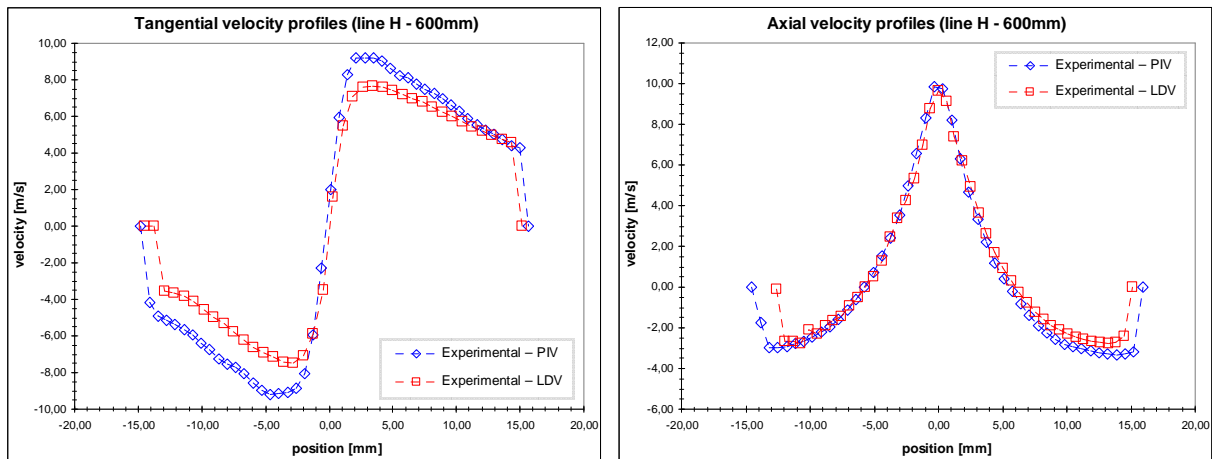


Figure 11. Tangential and axial velocity profiles measured with LDV and PIV techniques, station at  $z=600\text{mm}$ .

### 7. NUMERICAL RESULTS

Figure 12 shows the pressure contour at the central plane and an instantaneous velocity isosurface (velocity=7.5m/s) in the final section of the hydrocyclone (close to the underflow interface). The interesting features here are the low pressure core in the region around the hydrocyclone axis and the vortex precessing shown by the velocity isosurface.

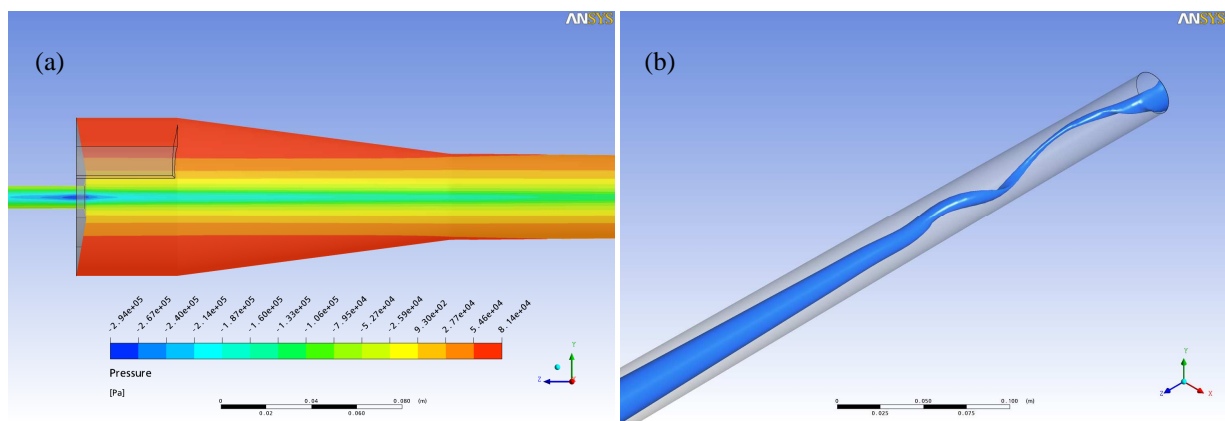


Figure 12. (a) Contours of pressure (central plane) and; (b) Velocity isosurface.

The velocity profiles are captured in the same position of the experimental stations. The comparison of the velocity profiles is shown in the next section.

### 8. COMPARISON AND CONCLUSIONS

The comparison among LDV, PIV and simulation velocity profiles is shown in Figs. 13, 14 and 15. In general, good agreement between measured data with LDV and PIV techniques was observed, even considering that each technique was used in different days (slightly different conditions). A higher deviation was observed in the tangential velocity profiles in the stations closer to the underflow (as seen in the plot for station at  $z=600\text{mm}$ ). We believe that this deviation was due to technical difficulties to acquire LDV data in that region (low curvature radius increasing reflections generating too much noise).

There is some uncertainty in the flow rate and split measured data. This is caused by the use of only one rotameter flowmeter (located in the feed line). This uncertainty prevented us from defining more precise values to the simulation boundary conditions. Even though, the comparison among experimental data and simulated results shows also a good agreement. The deviation observed in the velocity profiles can be reduced by using more refined meshes and prescribing more precise boundary conditions.

In the near future the group is improving the flow measuring devices (new equipment and measurements in all lines). New experimental data and new simulations will be performed at this time.

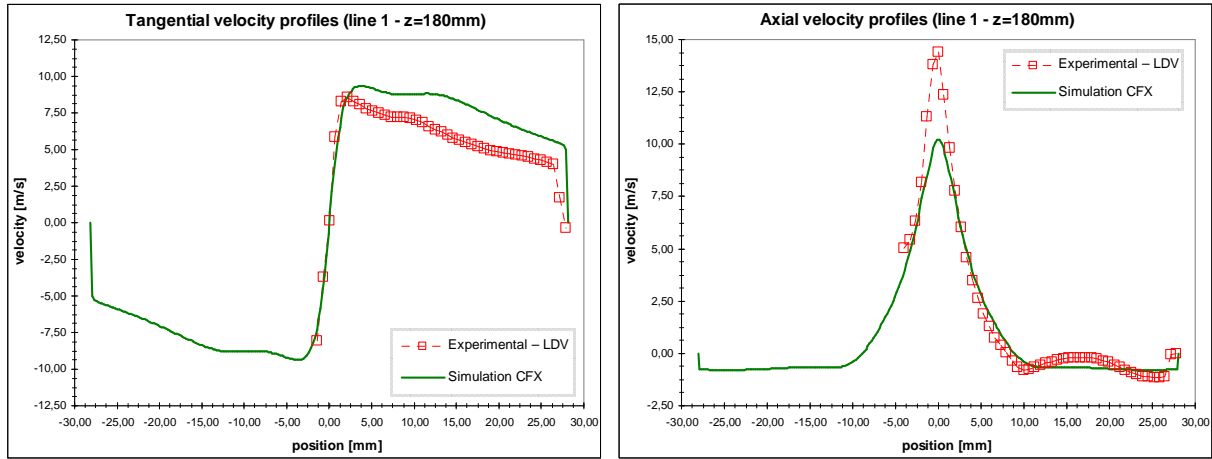


Figure 13. Tangential and axial velocity profiles measured with LDV and from simulation result, station at  $z=180\text{mm}$ .

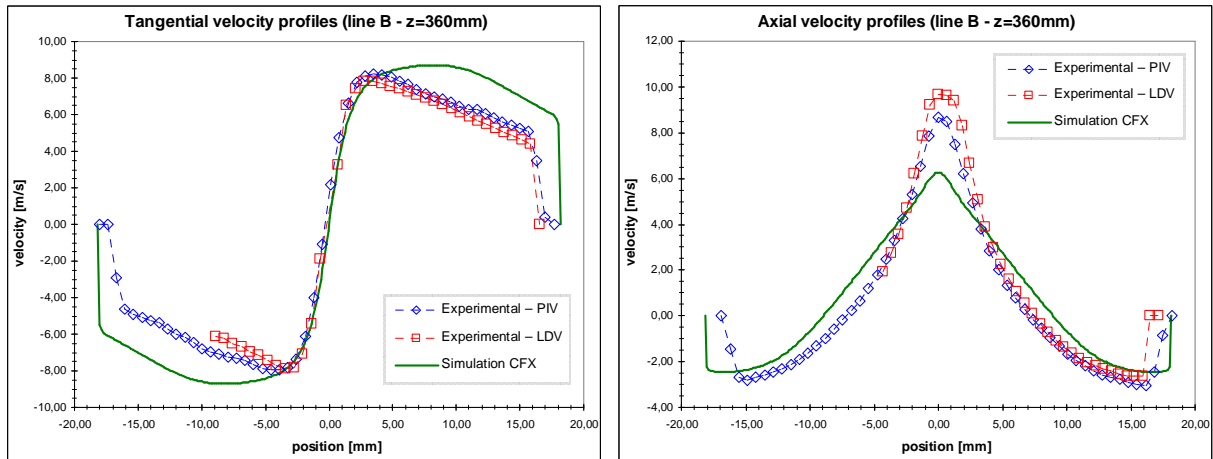


Figure 14. Tangential and axial velocity profiles measured with LDV, PIV and from simulation result, station at  $z=360\text{mm}$ .

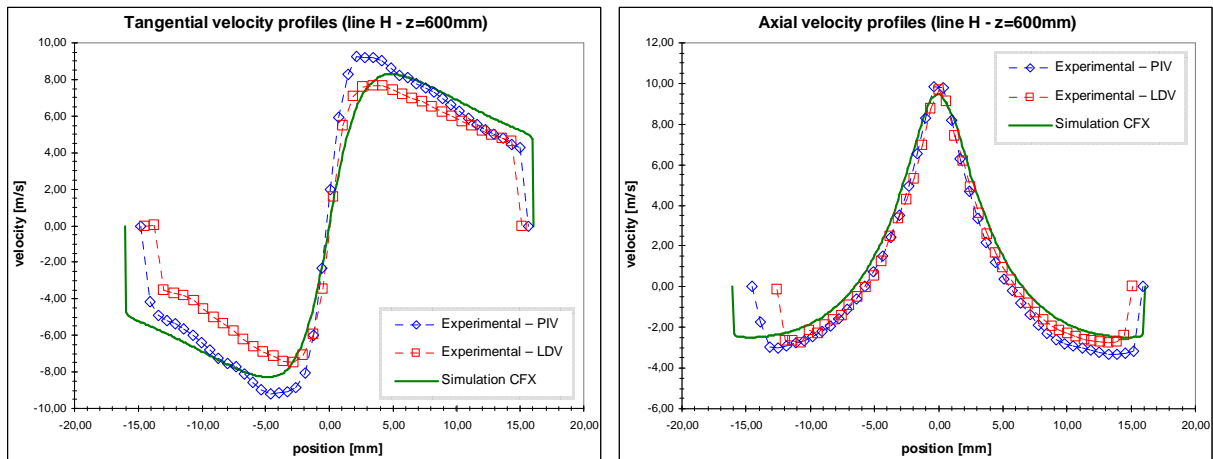


Figure 15. Tangential and axial velocity profiles measured with LDV, PIV and from simulation result, station at  $z=600\text{mm}$ .

Concluding, in spite of all the difficulties cited before, the results, both experimental and simulated, are very promising, and the data generated so far is being applied in new hydrocyclone designs and used to validate the numerical simulations.

This research will be complemented with field tests using steel prototypes of the new hydrocyclone designs above mentioned, operating with multiphase flows. In parallel simulation of the real operational conditions will be performed and validated with field data.



## 9. ACKNOWLEDGEMENTS

We must recognize PETROBRAS for providing the measuring equipment and computational cluster to perform this investigation.

## 10. REFERENCES

- Albrecht, H.E., Borys, M. Damaschke, N. and Tropea, C., 2003, “Laser Doppler and Phase Doppler Measurement Techniques”, Springer, Berlin, Germany
- Aguirre Oliveira Jr., J. A., Paladino, E., Reis, M., Moraes, C.A.C. de, Melo, D.C. de, 2006, “CFD Modeling of Hydrocyclone Flows”, Precedings of CFD-Oil 2006, Rio de Janeiro, Brazil.
- ANSYS CFX-11.0 Documentation, ANSYS Inc. 2007.
- LA Vision PIV Documentation, 2006, Göttingen, Germany
- Montavon, C.A., Grotjans, H., Hamill, I.S., Phillips, H.W. and Jones, I.P., 2000, “Mathematical Modelling and Experimental Validation of Flow in a Hydrocyclone”, BHR Conference on Cyclone Technologies, Warwick, England.
- Raffel, M., Willert, C. and Kompenhans, J., 1998, “Particle Image Velocimetry”, Springer, Berlin, Germany.
- Silva Freire, A.P., Ilha, A. and Colaço M.J., Editors, 2006, “Coleção Cadernos de Turbulência, Turbulência, Vol. 5, T. 1 and 2.
- Stanislas, M. Hinsch, K., Westerweel, J. and Schröder, A., 2007, Documentation of the 15<sup>th</sup> course “Application of Particle Image Velocimetry – Theory and Practice”, Göttingen, Germany
- TSI LDA System Documentation, 2005, Shoreview, USA
- Wieneke, B., 2005, “Stereo –PIV using selfcalibration on particle images”, 2005, Experiments in Fluids, Springer-Verlag, Berlin, Germany

## 11. RESPONSIBILITY NOTICE

The authors are the only responsible for the printed material included in this paper.